Dynamic Characteristic and Control of a Hypersonic Flight Vehicle

Dongsheng Qin, Qiangjun Zhu, Chenxi Wang
College of Astronautics, Northwestern Polytechnical University, Xi'an, China
qdsjungle@tom.com, wangchenxi_nwpu@163.com

Abstract - The longitudinal dynamics of hypersonic flight vehicles present an unstable phugoid mode and a new height mode. Hypersonic flight will be subject to attitude and height divergence that would require stabilizing feedback control. A method of design velocity and altitude tracking controller for hypersonic flight vehicles is outlined in this paper. The nonlinear longitudinal model of hypersonic flight vehicles is trimmed and linearized. With the aid of a full-state observer, the controller is designed follow the LQR method based on the linearized model. The simulation results show that the designed controller can be used for velocity and height tracking control.

Index Terms - hypersonic flight vehicle; tracking control; linear quadratic regulator (LQR)

1. INTRODUCTION

Hypersonic flight vehicles are defined as the vehicles whose normal flight speed excess 5 Mach. The renewed interest of developing hypersonic flight vehicles is based upon the advantages it offers, such as a possible solution to provide routing and affordable space access and high speed civil transportations [1]. However, there are some key technological obstacles to the feasibility of hypersonic flight, one of which is controller design [2]. The aerodynamic effects of hypersonic speeds, the integration of the airframe and the propulsion system, the extreme range of operating conditions and the rapid change of mass distribution, cause the flight dynamics of hypersonic flight vehicles completely differ from that of conventional aircrafts. Thus, it requires more careful consideration to design reliable and effective hypersonic flight vehicle controllers.

Because of the extreme complexity of the dynamics, most of the work on designing the controller for hypersonic vehicles only involves the longitudinal dynamics. While many work devoted to develop nonlinear controller design [3], this paper devoted to develop an LQR controller which is much easier to implement and more mature in reality. The nonlinear dynamics of hypersonic flight vehicle is linearized at a trim point, and then a controller is designed for the region near this trim point. The main objective is to determine the feasibility of linear control methods for the nonlinear dynamics of hypersonic flight vehicle via designs on linearized models. This method can be extended by gain scheduling at several trim points.

This paper is organized as follows. Section II presents the longitudinal dynamics model of a hypersonic flight vehicle. An Analysis of the flight dynamic characteristics of this model is presented in section III. Section IV gives the tracking controller design method for hypersonic flight vehicles and the simulation results of the controller a shown in Section V. Finally, the conclusion is presented in Section VI.

2. MODEL DESCRIPTION

The fifth-order longitudinal equations of motion for a hypersonic vehicle, which include both the centripetal acceleration that results from a curved flight path and in inverse square-law gravitational model, are shown as follows:

$$\dot{V} = \frac{T\cos\alpha - D}{m} - \frac{\mu\sin\gamma}{r^2} , \tag{1}$$

$$\dot{\gamma} = \frac{L + T\sin\alpha}{mV} - \frac{(\mu - V^2 r)\cos\gamma}{Vr^2} , \tag{2}$$

$$\dot{h} = V\sin\gamma , \tag{3}$$

$$\dot{\alpha} = q - \dot{\gamma} , \tag{4}$$

$$\dot{q} = M_y / I_y . \tag{5}$$

where V is the flight speed, α is the angle of attack, m is the mass, γ is the flight path angle, h is the height, q is the pitch rate, I_y is the inertial moment about y axis. The values of the lift L, drag D, thrust T, and pitching moment M_y are given, respectively, by

$$L = \frac{1}{2}\rho V^2 S C_L(h,V,\alpha,q,\delta_e,\delta_t) , \tag{6}$$

$$D = \frac{1}{2}\rho V^2 S C_D(h,V,\alpha,q,\delta_e,\delta_t) , \tag{7}$$

$$T = \frac{1}{2}\rho V^2 S C_T(h,V,\alpha,q,\delta_e,\delta_t) , \tag{8}$$

$$M_y = \frac{1}{2}\rho V^2 S\bar{c} C_M(h,V,\alpha,q,\delta_e,\delta_t) , \tag{9}$$

where S is reference area, $\bar{c}$ is mean aerodynamic chord length. The lift coefficient C_L, drag coefficient C_D, thrust coefficient C_T and pitch moment coefficient C_M are functions of height h, velocity V, angle of attack α, pitch

© 2013. The authors - Published by Atlantis Press

rate q, elevator deflection angle δ_e and throttle setting δ_t, and their explicit expressions can be found in [5]. The air density ρ, speed of sound a, and the radius from the Earth center r are modeled as functions of height h as

$$\rho = 1.2266 e^{-h/7315.2}, \tag{10}$$

$$a = 2.949475\times10^{-8} h^2 - 9.16\times10^{-4} h + 303.5808, \tag{11}$$

$$r = h + 6356766. \tag{12}$$

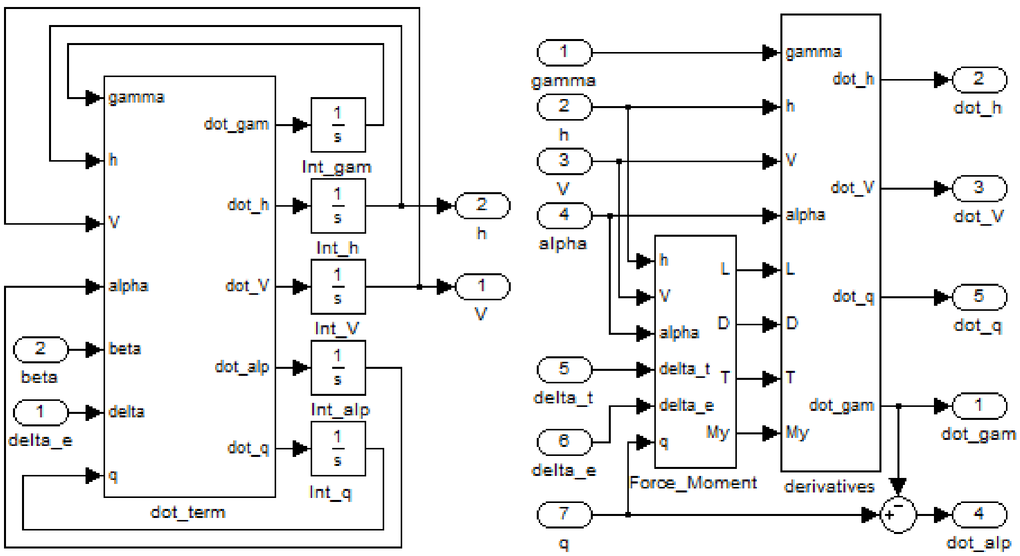

Fig. 1 Simulink model of longitudinal equations of motion for hypersonic vehicle: (a) top level of the model, (b)second level of the model.

$$\mathbf{A}_p = \begin{bmatrix} 0.000017877879 & -0.000000284736 & 0 & -14.784614786109 & -9.704014719072 \\ 0 & 0 & 0 & 0 & 4590.300040256541 \\ 0.000017715521 & -0.000000282150 & -0.068199641886 & 0.590394992515 & 4590.300040256541 \\ -0.000000857948 & 0.000000189240 & 1.000000000000 & -0.043988770414 & 0 \\ 0.000000857948 & -0.000000189240 & 0 & 0.043988770414 & 0 \end{bmatrix}$$

$$\mathbf{B}_p = \begin{bmatrix} 0 & 8.319765289527279 \\ 0 & 0 \\ 3.316269764212172 & 0 \\ 0 & -0.000057525209151 \\ 0 & 0.000057525209151 \end{bmatrix}, \quad \mathbf{C}_p = \begin{bmatrix} 1 & 0 & 0 & 0 & 0 \\ 0 & 1 & 0 & 0 & 0 \end{bmatrix}$$

Fig. 2 Matrices of the plant state-space model.

3. Flight Dynamic Characteristics

Fig. 1 shows a Simulink model of the longitudinal equations of motion for the hypersonic vehicle. This Simulink model can be used to get the trim point by invoking the Matlab function "trim". The vehicle is trimmed at $V = 4590.3$ m/s, $h = 33528$ m, $\alpha = 0.0317$ rad, $\delta_t = 0.177$ rad, and $\delta_e = -0.0070$ rad. Then, a numerical state-space model is obtained by invoking the Matlab function "linmod" with the Simulink model and trim point as input parameters. The state-space model can be described by

$$\begin{cases} \dot{\boldsymbol{x}}_p = \mathbf{A}_p \boldsymbol{x}_p + \mathbf{B}_p \boldsymbol{u}_p, \\ \boldsymbol{y}_p = \mathbf{C}_p \boldsymbol{x}_p, \end{cases} \tag{13}$$

where

$\boldsymbol{x}_p = [V \quad h \quad \gamma \quad \alpha \quad q]^T$, $\boldsymbol{u}_p = [\delta_e \quad \delta_t]^T$, $\boldsymbol{y}_p = [V \quad h]^T$, and the numerical values of system matrix $\mathbf{A}_p$, input matrix $\mathbf{B}_p$ and output matrix $\mathbf{C}_p$ are shown in Fig. 2.

Fig. 3 is a pole-zero map of the state-space model described by(13). There are five characteristic roots of the longitudinal motion of hypersonic vehicle in Fig. 3. Two bigger real eigenvalues -0.825 and 0.712 represent a statically unstable short-period mode. A pair of conjugate complex eigenvalues $-3.38\times10^{-5} \pm 0.0278\,i$ portrays a lightly damped phugoid mode. A small real eigenvalue 0.000485 indicates a mildly unstable height mode. Consequently, hypersonic cruising flight would be subject to attitude and height divergence that would require stabilizing feedback control.

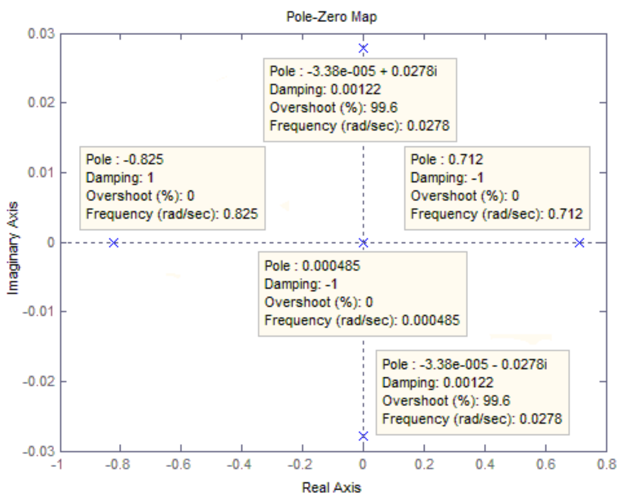

Fig. 3 Zero-pole map of system(13).

4. Controller Design

A. LQ Controller

The objective is to control the velocity and altitude of the hypersonic flight vehicle to follow a reference command, using control inputs such as elevator deflection, and the engine throttle. This will be done by designing full-state feedback controllers to achieve velocity and altitude tight tracking in the neighborhood of a trim condition.

To increase model accuracy, a simple model of actuator dynamics can be added to the plant model as follows [7]:

$$\dot{\boldsymbol{x}}_\delta = \mathbf{A}_\delta \boldsymbol{x}_\delta + \mathbf{B}_\delta \boldsymbol{u}_\delta \,, \tag{14}$$

where

$$\mathbf{A}_\delta = \begin{bmatrix} -20 & 0 \\ 0 & -10 \end{bmatrix},\ \mathbf{B}_\delta = \begin{bmatrix} 20 & 0 \\ 0 & 10 \end{bmatrix},$$

$$\boldsymbol{x}_\delta = \boldsymbol{u}_p = \begin{bmatrix} \delta_e \\ \delta_t \end{bmatrix},\ \boldsymbol{u}_\delta = \begin{bmatrix} u_{\delta e} \\ u_{\delta t} \end{bmatrix}.$$

After appending the actuator dynamics (14) to the plant model(13), we obtain a new system as follows:

$$\begin{cases} \dot{\boldsymbol{x}}_1 = \mathbf{A}_1 \boldsymbol{x}_1 + \mathbf{B}_1 \boldsymbol{u}_1 \,, \\ \boldsymbol{y}_1 = \mathbf{C}_1 \boldsymbol{x}_1 \,, \end{cases} \tag{15}$$

where

$$\mathbf{A}_1 = \begin{bmatrix} \mathbf{A}_p & \mathbf{B}_p \\ \mathbf{0} & \mathbf{A}_\delta \end{bmatrix},\ \mathbf{B}_1 = \begin{bmatrix} \mathbf{0} \\ \mathbf{B}_\delta \end{bmatrix},\ \mathbf{C}_1 = \begin{bmatrix} \mathbf{C}_p & \mathbf{0} \end{bmatrix}, \boldsymbol{x} = \begin{bmatrix} \boldsymbol{x}_p \\ \boldsymbol{x}_\delta \end{bmatrix},$$
$$\boldsymbol{u}_1 = \boldsymbol{u}_\delta \,.$$

For the model described by(15), the tacking controller design objective is to design the control signal $\boldsymbol{u}$ to achieve zero output tracking error, which is defined as

$$\boldsymbol{e} = \boldsymbol{y}_1 - \boldsymbol{y}_d = [V - V_d \quad h - h_d]^T \,. \tag{16}$$

This tracking problem will be converted to a regulator problem as illustrated below.

The integral tracking error is given by

$$\boldsymbol{x}_2 = \int_0^t \boldsymbol{e}(\tau)\,\mathrm{d}\tau \,. \tag{17}$$

It can be appended to system(15), and the augmented system can be written by

$$\begin{cases} \dot{\boldsymbol{x}} = \mathbf{A}\boldsymbol{x} + \mathbf{B}\boldsymbol{u} + \boldsymbol{G}\boldsymbol{y}_d \,, \\ \boldsymbol{y} = \mathbf{C}\boldsymbol{x} \,, \end{cases} \tag{18}$$

where

$$\mathbf{A} = \begin{bmatrix} \mathbf{A}_1 & \mathbf{0} \\ \mathbf{C}_1 & \mathbf{0} \end{bmatrix},\ \mathbf{B} = \begin{bmatrix} \mathbf{B}_1 \\ \mathbf{0} \end{bmatrix}, \mathbf{G} = \begin{bmatrix} \mathbf{0} \\ -\mathbf{I} \end{bmatrix},$$

$$\mathbf{C} = \begin{bmatrix} \mathbf{C}_1 & \mathbf{0} \end{bmatrix},\ \ \boldsymbol{x} = \begin{bmatrix} \boldsymbol{x}_1 \\ \boldsymbol{x}_2 \end{bmatrix},\ \boldsymbol{u} = \boldsymbol{u}_1,\ \boldsymbol{y} = \boldsymbol{y}_1 \,.$$

Let the steady-state values be denoted by overbars and deviation from the steady-state values by tildes, then

$$\begin{cases} \tilde{\boldsymbol{x}} = \boldsymbol{x} - \bar{\boldsymbol{x}}, \tilde{\boldsymbol{u}} = \boldsymbol{u} - \bar{\boldsymbol{u}}, \\ \tilde{\boldsymbol{y}} = \boldsymbol{y} - \bar{\boldsymbol{y}}, \tilde{\boldsymbol{e}} = \boldsymbol{e} - \bar{\boldsymbol{e}} = \boldsymbol{e}. \end{cases} \tag{19}$$

The dynamics of the deviation system are

$$\begin{cases} \dot{\tilde{\boldsymbol{x}}} = \mathbf{A}\tilde{\boldsymbol{x}} + \mathbf{B}\tilde{\boldsymbol{u}} \,, \\ \tilde{\boldsymbol{y}} = \mathbf{C}\tilde{\boldsymbol{x}} \,, \end{cases} \tag{20}$$

where the deviation $\tilde{\boldsymbol{y}}$ is equal to $\tilde{\boldsymbol{e}}$

$$\tilde{\boldsymbol{y}} = \tilde{\boldsymbol{y}}_1 = \boldsymbol{y}_1 - \bar{\boldsymbol{y}}_1 = \boldsymbol{y}_1 - \boldsymbol{y}_d = \boldsymbol{e} = \boldsymbol{e} - \boldsymbol{0} = \tilde{\boldsymbol{e}}. \tag{21}$$

According to the LQR control structure, the control design problem is to find control inputs to minimize the performance index function defined as

$$J = \frac{1}{2}\int_0^\infty \left(\tilde{\boldsymbol{x}}^T \mathbf{Q}\tilde{\boldsymbol{x}} + \tilde{\boldsymbol{u}}^T \mathbf{R}\tilde{\boldsymbol{u}}\right)\mathrm{d}t \,. \tag{22}$$

where $\mathbf{Q}$ is a real symmetric positive semi-definite matrix, $\mathbf{R}$ is a real symmetric positive definite matrix.

Using the standard method, the optimal feedback control vector is given by

$$\tilde{\boldsymbol{u}} = -\mathbf{K}\tilde{\boldsymbol{x}}, \tag{23}$$

where the full state feedback control gain matrix is

$$\mathbf{K} = \mathbf{R}^{-1}\mathbf{B}^{T}\mathbf{P}, \tag{24}$$

and the matrix $\mathbf{P}$ is the positive-definite solution of the algebraic Riccati equation:

$$\mathbf{A}^{T}\mathbf{P} + \mathbf{PA} - \mathbf{PBR}^{-1}\mathbf{B}^{T}\mathbf{P} + \mathbf{Q} = 0. \tag{25}$$

B. State Observer

Until now, we assume that the state variables can be obtained from measure instruments and design LQR controller directly. In reality, the state variables cannot be determined exactly from the measure instruments, so they must be estimated. A device performing an estimate of the state variables is known as an observer, and it can be expressed in the following form

$$\dot{\hat{\boldsymbol{x}}}_1 = \mathbf{A}_1\hat{\boldsymbol{x}}_1 + \mathbf{B}_1\boldsymbol{u}_1 + \mathbf{L}\left[\boldsymbol{y}_1 - \mathbf{C}_1\hat{\boldsymbol{x}}_1\right], \tag{26}$$

where $\hat{\boldsymbol{x}}_1$ is the observer state vector and $\mathbf{L}$ is an observer gain matrix. Subtracting (15) from (26), we obtain the dynamics of estimate error

$$\dot{\boldsymbol{x}}_1 - \dot{\hat{\boldsymbol{x}}}_1 = \left[\mathbf{A}_1 - \mathbf{LC}_1\right]\left(\boldsymbol{x}_1 - \hat{\boldsymbol{x}}_1\right). \tag{27}$$

The objective is to find a matrix $\mathbf{L}$ such that the observer state vector $\hat{\boldsymbol{x}}_1$ approaches the state $\boldsymbol{x}_1$ as time increases. This amounts to determining $\mathbf{L}$ so that all the eigenvalues of the matrix $\mathbf{A}_1 - \mathbf{LC}_1$, known as observer poles, lie in the left half of the complex plane. In implementing feedback controls, we must use the estimated state vector $\hat{\boldsymbol{x}}_1$ to replace the state vector $\boldsymbol{x}_1$. The optimal feedback control vector is obtained using the deviation state vector $\tilde{\boldsymbol{x}}$. While the deviation $\tilde{\boldsymbol{x}}_2$ can be simply calculated by integrating the tracking error $\boldsymbol{e}$, the deviation $\tilde{\boldsymbol{x}}_1$ is more complex to obtain. When system $\left(\mathbf{A}_1, \mathbf{B}_1, \mathbf{C}_1\right)$ is steady, the derivatives of the state is equal to zero and the output is equal to the desired values, that is, the steady-state values denoted by overbars can be obtained as follows:

$$\begin{bmatrix} \bar{\boldsymbol{x}} \\ \bar{\boldsymbol{u}}_1 \end{bmatrix} = \begin{bmatrix} \mathbf{A}_1 & \mathbf{B}_1 \\ \mathbf{C}_1 & \mathbf{0} \end{bmatrix}^{-1} \begin{bmatrix} \mathbf{0} \\ \boldsymbol{y}_d \end{bmatrix} = \begin{bmatrix} \mathbf{H}_{11} & \mathbf{H}_{12} \\ \mathbf{H}_{21} & \mathbf{H}_{22} \end{bmatrix} \begin{bmatrix} \mathbf{0} \\ \boldsymbol{y}_d \end{bmatrix}. \tag{28}$$

Thus the deviation $\tilde{\boldsymbol{x}}_1$ can be estimated by

$$\hat{\tilde{\boldsymbol{x}}}_1 = \hat{\boldsymbol{x}}_1 - \bar{\boldsymbol{x}}_1, \tag{29}$$

hence,

$$\tilde{\boldsymbol{u}} = -\mathbf{K}\tilde{\boldsymbol{x}} = -\left[\mathbf{K}_1 \quad \mathbf{K}_2\right]\left[\hat{\boldsymbol{x}}_1 - \mathbf{H}_{12}\boldsymbol{y}_d \quad \tilde{\boldsymbol{x}}_2\right]^{T}. \tag{30}$$

Fig. 4 is the block diagram of the designed LQR controller with full state observer.

5. Simulation Results

The control objective is to achieve a simultaneous tracking of velocity and altitude command. The deviations $350\,\text{m/s}$ for V, and $3500\,\text{m}$ for h from the trim state are reasonable, due to the maneuverability requirements for hypersonic flight vehicle. The desired command signals V_d and h_d were generated by passing the velocity and height step signals through a filter

$$P(s) = \frac{\omega_n^2}{s^2 + 2\zeta\omega_n s + \omega_n^2}, \tag{31}$$

where ζ is the damping coefficient and ω_n is the natural frequency of the filter.

Fig. 5 and Fig. 6 show the transient response of the outputs V and h to a commanded step change in the velocity and altitude. It can be seen that the controller work well to provide asymptotic tracking of velocity and height with no significant overshot or steady state error. Fig. 7 and Fig. 8 present time history of the elevator deflection and engine throttle response. It shows that both control input are within the actuator saturation limit. However, it should be kept in mind that tuning the weighting matrices of the LQR problem for controllers can vastly alter the resulting performance.

6. Conclusion

This paper presents a control method used in designing the velocity and height tracking control law for a hypersonic flight vehicle. A simulation of the LQR controller design is presented, which uses the linearized longitudinal dynamics about a trimmed point in steady-state flight. The simulation results verified that the designed controller can be used to for velocity and height tracking control.

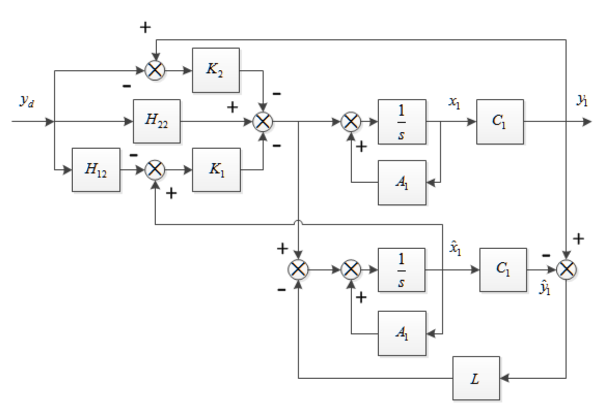

Fig. 4 The designed controller.

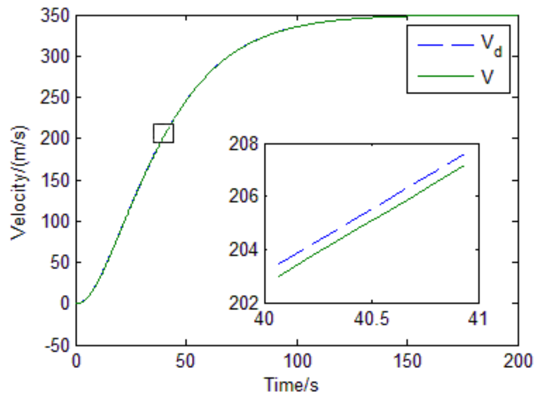

Fig. 5 Velocity response.

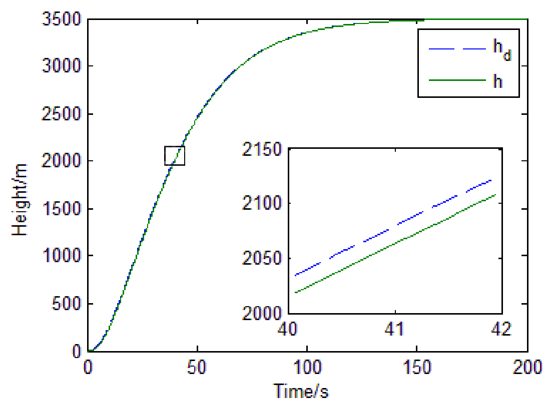

Fig. 6 Height response.

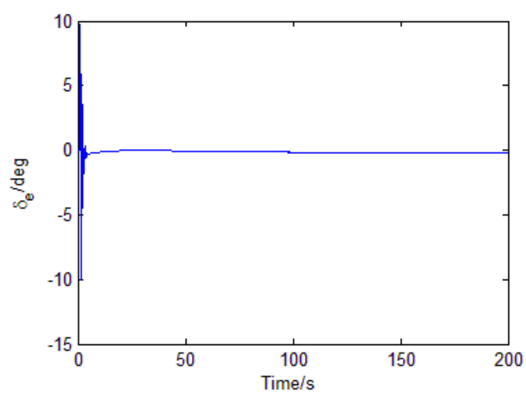

Fig. 7 Input of elevator deflection angle .

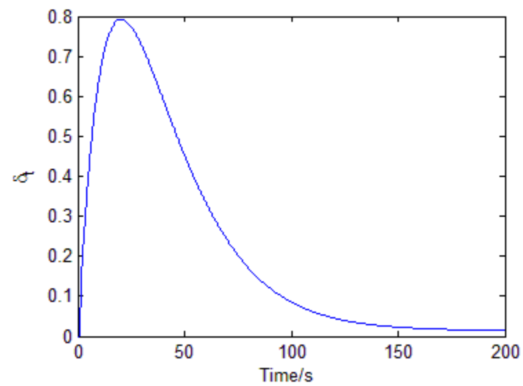

Fig. 8 Input of engine throttle setting.

REFERENCES

[1] A. Clark, C. Wu, M. Mirmirani, S. Choi, and M. Kuipers, "Development of an airframe-propulsion integrated generic hypersonic vehicle model," Proc. 44th AIAA Aerospace Sciences Meeting and Exhibit, Reno, Nevada, Jan. 2006.

[2] B. Fidan, M. Mirmiran, P. A. Ioannou, and J. Clerk Maxwell, "Flight dynamics and control of air-breathing hypersonic vehicles: review and new directions," Proc. 12th AIAA International Space Planes and Hypersonic Systems and Technologies, Norfolk, Virginia, Dec. 2003.

[3] H. P. Lee, S. E. Reiman, C. H. Dillon, and H. M. Youssef, "Robust nonlinear dynamic inversion control for a hypersonic cruise vehicle," Proc. AIAA Guidance, Navigation and Control Conference and Exhibit, Hilton Head, South Carolina, Aug. 2007.

[4] F. Poulain, H. P. Lahanier, and L. Serre, "Nonlinear control of a airbreathing hypersonic vehicle," Proc. 16th AIAA/DLR/DGLR International Space Planes and Hypersonic Systems and Technologies Conference, Bremen, Germany, Oct, 2009.

[5] Q. Wang, and R. F. Stengel, "Robust nonlinear control of a hypersonic aircraft," Journal of guidance, control, and dynamics, vol. 23, pp. 577-585, July-August 2000.

[6] Y. B. Liu, "Research on modeling and advanced flight control theories for hypersonic vehicle," Nanjing, China: Nanjing University, March. 2007.

[7] K. P. Groves, D. O. Sigthorsson, A. Serrani, S. Yurkovich, M. A. Bolender, and D. B. Doman, "Reference command tracking for a linearized model of an air-breathing hypersonic vehicle," Proc. AIAA Guidance, Navigation, and Control Conference and Exhibit, San Francisco, California, 2005.

[8] C, K, Lu, and J. Yan., "Optimal PIF-LQR control design for a generic hypersonic vehicle," Computor Simulation, Vol. 26, pp. 84-87, May 2009.